# Low-Dimensional Chaotic Attractors in Drift-Wave Turbulence

M. Persson

*Department of Theoretical Physics and Plasma Research Laboratory, Research School of Physical Sciences, The Australian National University, G.P.O. Box 4, Canberra, Australian Capital Territory 2601, Australia*

H. Nordman

*Institute for Electromagnetic Field Theory and EURATOM/NFR Association, Chalmers University of Technology, S-41296 Göteborg, Sweden*

(Received 3 June 1991)

Simulation results of toroidal $\eta_i$-mode turbulence are analyzed using mathematical tools of nonlinear dynamics. Low-dimensional chaotic attractors are found in the strongly nonlinear regime while in the weakly interacting regime the dynamics is high dimensional. In both regimes, the solutions are found to display sensitive dependence on initial conditions, characterized by a positive largest Liapunov exponent.

PACS numbers: 52.35.Ra, 05.45.+b, 52.35.Kt

In 1963, Lorenz [1], and later Ruelle and Takens [2], suggested that the transition to fluid turbulence can be initiated by strange (chaotic) attractors. Since then, a number of results have been reported in support of this scenario. For example, turbulent solutions of the Navier-Stokes equations have shown low-dimensional chaotic features [3]. Furthermore, experimental evidence has been presented for the presence of low-dimensional chaotic attractors in certain hydrodynamic systems, like, e.g., in Couette-Taylor flow [4] and in Rayleigh-Bénard convection [5]. Chaotic behavior and period doubling have also been observed in pulsed plasma discharges [6].

Fluctuation-driven particle and energy transport are considered to represent major obstacles in the striving for achieving thermonuclear fusion in magnetically confined plasmas. During the last decade, a considerable amount of work has been done trying to correlate the experimentally observed transport with predictions based on various nonlinear drift-wave and magnetohydrodynamic models [7]. In present day high-temperature tokamak experiments, the temperature-gradient-driven drift waves have attracted a strong interest. Among these, the interchangelike toroidal $\eta_i$ mode [8–10] ($\eta_i = d\ln T_i/d\ln n_i$), which is driven by the combined effects of the ion temperature gradient and the magnetic-field curvature, is considered as one of the serious candidates for explaining the anomalous ion heat loss in tokamaks.

In this Letter, fluid simulations of toroidal $\eta_i$-mode turbulence are analyzed in the context of nonlinear dynamics. The correlation dimension is calculated for a range of equilibrium parameters. In addition, to characterize the chaotic motion on the attractor, the largest Liapunov exponent is calculated by following the exponential separation of nearby orbits in phase space. For the first time, simulation results are presented indicating that for certain tokamak equilibria the drift-wave dynamics is characterized by low-dimensional chaotic attractors. In these configurations, a few active degrees of freedom, rather than the infinite number of modes associated with the fully developed turbulence, are responsible for the transport.

The model used is an improved two-dimensional (i.e., in the poloidal plane), hydrodynamic ion model [11], valid for arbitrary $L_n/L_B$ (the scale length of the density and the magnetic-field gradients), together with an adiabatic electron response. Combining the ion continuity and energy equations gives the following nonlinear evolution equations for the perturbed electrostatic potential $\phi$ and ion temperature $T$ [12]:

$$(1-\nabla^2)\frac{\partial\phi}{\partial t} = -\left[1-\varepsilon_n\left(1+\frac{1}{\tau}\right)+\frac{1+\eta_i}{\tau}\nabla^2\right]\frac{\partial\phi}{\partial y} + \varepsilon_n\frac{\partial T}{\partial y}+[\phi,\nabla^2\phi]\,, \tag{1}$$

$$\frac{\partial T}{\partial t} = -\left[\frac{\eta_i}{\tau}+\frac{2}{3\tau}\left(1+\frac{1+\eta_i}{\tau}\right)\nabla^2\right]\frac{\partial\phi}{\partial y} + \frac{2\varepsilon_n}{3\tau}\left(1+\frac{1}{\tau}\right)(1+\nabla^2)\frac{\partial\phi}{\partial y} + \frac{\varepsilon_n}{3\tau}(7+2\nabla^2)\frac{\partial T}{\partial y}-[\phi,T]+\frac{2}{3\tau}[\phi,\nabla^2\phi]\,, \tag{2}$$

where $\varepsilon_n = 2L_n/L_B$, $\eta_i = L_n/L_{T_i}$, and $\tau = T_e/T_i$. In Eqs. (1) and (2) we have used the dimensionless variables $(x,y)\rightarrow\rho_s(x,y)$ and $t\rightarrow L_n t/c_s$, where $c_s=(T_e/m_i)^{1/2}$, $\rho_s = c_s/\Omega_{ci}$, $\Omega_{ci}=eB/mc$, and where $(x,y)$ represents coordinates in the radial and poloidal direction. The fields have been normalized as

$$\phi = \frac{e\Phi}{T_e}\frac{L_n}{\rho_s}\,,\quad T=\frac{\delta T_i}{T_e}\frac{L_n}{\rho_s}\,.$$

The model includes first-order finite-Larmor-radii effects (FLR), polarization drift effects, and compressibility due to field curvature. For simplicity, parallel ion dynamics and magnetic shear have been neglected in the present study. The dominant nonlinearities arise from the $\mathbf{E}\times\mathbf{B}$ convection and we have $\mathbf{v}_E\cdot\nabla f=\hat{\mathbf{z}}\cdot\nabla\phi\times\nabla f\equiv[\phi,f]$. The

simulations (for details see Ref. [12] and references therein) were performed on a $64\times64$ grid spanning $-2.25 \le k_x\rho_s, k_y\rho_s \le 2.25$, using a fully dealiased spectral method. In the simulations, each field is artifically damped at high and low $k$ [13] to represent the effect of high-$k$ viscosity and low-$k$ ion Landau damping, respectively, i.e., we have $\gamma=\gamma_0(1-k_\perp^2/k_0^2)$ for $k \le k_0$ and $\gamma=\gamma_\infty$ at $k \ge k_\infty$ with typically $k_0=0.5$, $\gamma_0=0.6$, $k_\infty=1.5$, $\gamma_\infty=2$ used in the simulations. The turbulence level and transport are largely insensitive to the high-$k$ dissipation whereas the dependence on the low-$k$ dissipation rates are stronger (see, e.g., Ref. [12]). However, for reasonable values, the chaotic features studied in this paper are only weakly dependent on $\gamma_0$.

The linear theory can provide useful indications of what to expect from the nonlinear simulations. Neglecting the convective nonlinearities in Eqs. (1) and (2), a quadratic dispersion relation is obtained [11], which in the limit $k\rho_s/\varepsilon_n \ll 1$ gives the real part of the frequency and the growth rate as

$$\omega_r=\frac{1}{2}\omega_{*e}\left\{1-\varepsilon_n\left(1+\frac{10}{3\tau}\right)-k^2\rho_s^2\left[1+\frac{1+\eta_i}{\tau}-\varepsilon_n\left(1+\frac{5}{3\tau}\right)\right]\right\}, \quad (3)$$

$$\gamma=\frac{(\varepsilon_n/\tau)^{1/2}}{1+k^2\rho_s^2}\omega_{*e}(\eta_i-\eta_{i\text{th}})^{1/2},$$

where $\omega_{*e}$ is the electron diamagnetic drift frequency and where the threshold $\eta_i$ value is

$$\eta_{i\text{th}}=\frac{1}{2}\left(\frac{4}{3}-\tau\right)+\frac{1}{4}\varepsilon_n\left(\tau+\frac{40}{9\tau}\right)+\frac{\tau}{4\varepsilon_n}-\frac{k^2\rho_s^2}{2\varepsilon_n}\left[\frac{5}{3}-\frac{\tau}{4}+\frac{\tau}{4\varepsilon_n}-\left(\frac{10}{3}+\frac{4}{\tau}-\frac{10}{9\tau}\right)\varepsilon_n+\left(\frac{5}{3}+\frac{\tau}{4}-\frac{10}{9\tau}\right)\varepsilon_n^2\right]. \quad (4)$$

Thus, the mode propagates in the ion diamagnetic drift direction (i.e., in the negative $\hat{y}$ direction) for $\varepsilon_n \ge 0.2$ ($\omega_r<0$), and the real part of the frequency is only weakly dependent on $\eta_i$ through the FLR term. In a region above marginal stability and with $\varepsilon_n \ge 0.5$ we have $\omega_r > \gamma$ and the turbulence is defined as weak [14]. In this regime, corresponding to the main part of the good confinement region in tokamaks, a good agreement between quasilinear ion heat fluxes and nonlinear simulation results have been obtained [12]. For $\varepsilon_n \approx 0.2$ ($\omega_r \approx 0$) on the other hand, a strong fluidlike instability with $\gamma \ge \omega_r$ develops even close to marginal stability. Here the quasilinear approximation is not applicable.

The $\eta_i$-$\varepsilon_n$ stability boundary for the fastest growing mode ($k^2\rho_s^2=0.1$) is given in Fig. 1. For flat density profiles ($\varepsilon_n$ large), the stability threshold is independent of $L_n$ and onset of instability requires only a sufficiently steep ion temperature gradient. Here, the turbulence is expected to be weak. This regime is particularly relevant to $H$-mode discharges and also to $L$-mode plasmas close to the $q=1$ surface where the density profile is relatively flat. In the edge region on the other hand, $\varepsilon_n$ is small and the model suggests a strongly nonlinear regime.

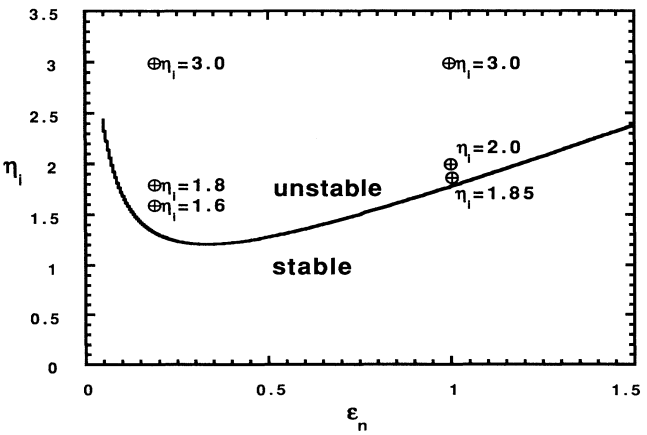


FIG. 1. The linear stability boundary in the $\eta_i$-$\varepsilon_n$ plane with $\tau=1$ and $k^2\rho_s^2=0.1$.

The time evolution of a single degree of freedom, such as a Fourier mode of the potential perturbations, is used to reconstruct the attractor utilizing an embedding technique [15]. In this procedure, a $D_e$-dimensional orbit is constructed from the vectors $\{\tilde{\phi}_k(t),\tilde{\phi}_k(t+\tau),\ldots,\tilde{\phi}_k(t+(D_e-1)\tau)\}$, where $\tilde{\phi}$ is taken as the real part of the potential $\phi$ in the nonlinearly saturated state after the initial transients have died away. For a sufficiently large embedding dimension $D_e$ and for a set of values of the delay time $\tau$ the Liapunov exponent and the correlation dimension are found to converge. Using the technique of Grassberger and Procaccia [16], the correlation dimension

$$D=\lim_{r\to 0}\frac{\ln[C(r)]}{\ln r} \quad (5)$$

is obtained from the slope of $\ln[C(r)]$ vs $\ln r$. The correlation sum $C(r)$, the number of pairs whose separation distance is less than $r$ over the number of pairs, in the limit of a densely covered attractor, approximates the probability that two points on the attractor are separated by a distance less than $r$. The limit $r \to 0$ is obtained by increasing the number of data points until $C(r)$ converges.

Examples of some correlation dimensions calculated using this technique are shown in Fig. 2, where they have been plotted versus the embedding dimension. The different cases plotted, which are marked in Fig. 1, were carried out using 25000 data points obtained from the simulations and with a delay of 10. Note that the small-$\varepsilon_n$ cases are low dimensional while the large-$\varepsilon_n$ cases have

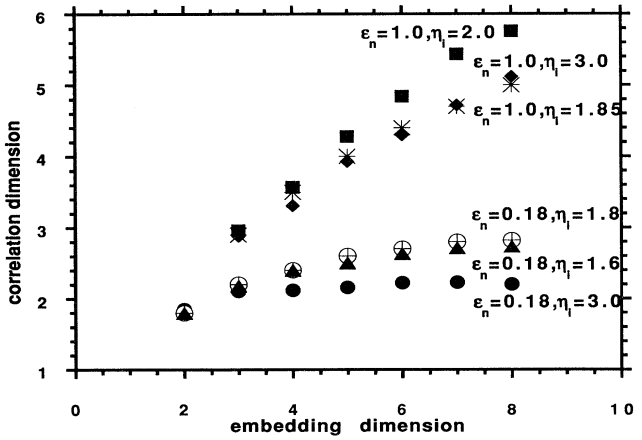


FIG. 2. The correlation dimension vs the embedding dimension calculated from 25000 points with a delay of 10.

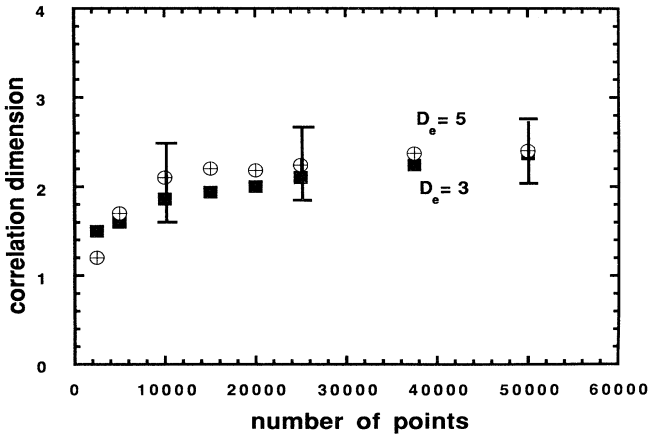


FIG. 3. The correlation dimension vs the number of points on the attractor for two different embedding dimensions $D_e$.

higher dimensions (the latter are not found to converge within the computational limits). Hence, for equilibria with $\gamma \geq \omega_r$ where the nonlinear interaction is expected to be strong, the dynamics is low dimensional, while in the weak coupling limit $\omega_r > \gamma$, the attractor is of higher dimension. This suggests that the coupling between the modes play an important role in determining whether the dynamics is high or low dimensional. The conclusion is supported by the observation that for equilibria with the same $\varepsilon_n$, an increased $\eta_i$, resulting linearly in an increased $\gamma/\omega_r$ and nonlinearly in higher saturated fluctuation levels, may locally result in an attractor of lower dimension. The latter is apparent in the low-dimensional low-$\varepsilon_n$ cases in Fig. 2 where the $\eta_i = 3$ case has a lower dimension and a higher $\gamma_r/\omega_r$ ratio than the cases with $\eta_i = 1.8$ and 1.6.

A close examination of the correlation dimension suggests that the low-dimensional attractors are fractals with correlation dimensions less than 3. To some extent the results presented in this Letter are consistent with observations in fluid dynamics where low-dimensional chaotic attractors are observed [4,5] in situations with strong nonlinear coupling.

The question of convergence and reliability in the dimension measurements is obviously of prime importance. The convergence with respect to the number of points on the attractor is exemplified in Fig. 3 where the correlation dimension is plotted versus the number of points for two different embedding dimensions $D_e$ for $\eta_i = 3$, $\varepsilon_n = 0.18$, and a delay of 10. Note the decreasing difference between the $D_e = 3$ and $D_e = 5$ cases as the number of points on the attractor increases. The correlation dimension as given by Eq. (5) gives a value averaged over the attractor. In order to determine the uncertainty and spread of values over the attractor the standard deviation of the pointwise correlation dimensions has been calculated. The results are indicated by the error bars in Fig. 3. Note that while decreasing with increasing number of data points the standard deviation (0.37 in comparison with the averaged value of 2.40) is fairly large even with 50000 data points. Takens's theorem [15] states that, except for unfortunate choices, the embedding is independent of the delay. However, for practical purposes it is obvious that too large and too small delays give poor results and only a relatively narrow set of delays are appropriate. We have found a delay of 10 to be a good choice for the calculations. The nonsaturated curves for the high-dimensional cases might actually saturate at relatively low values of the correlation dimension ($D < 10$) if a sufficient number of points could be handled. However, due to the extensive computations involved, both in the data generating simulations and during the correlation calculations, this is not feasible. We have therefore adopted the terminology that a system is low dimensional if it shows a clear sign of convergence when the number of points used in the calculation, restricted by the computer time, equals $10^{D_e}$.

To investigate the chaoticity or sensitive dependence on initial conditions, for these attractors, we compute the largest Liapunov characteristic exponent using an algorithm similar to that by Wolf *et al.* [17]. Starting from an initial point on the attractor $\{\tilde{\phi}_k(t_0), \tilde{\phi}_k(t_0+\tau), \ldots, \tilde{\phi}_k(t_0+(D_e-1)\tau)\}$ and finding the distance to the nearest neighbor, $L(t_0)$, it is propagated to a time $t_1$ when the initial length has evolved to length $L'(t_1)$. Using a replacement point and repeating this procedure we obtain an estimation of the maximum Liapunov exponent as

$$\lambda_1 = \frac{1}{t_m - t_0} \sum_{k=1}^{M} \ln \frac{L'(t_k)}{L(t_{k-1})}, \tag{6}$$

where $M$ is the number of replacement steps. Using files of up to 50000 data points in eight-dimensional reconstructions of the attractor, a positive maximum Liapunov exponent was found in all examined cases. Hence, the low-dimensional attractors observed for low $\varepsilon_n$ are chaot-

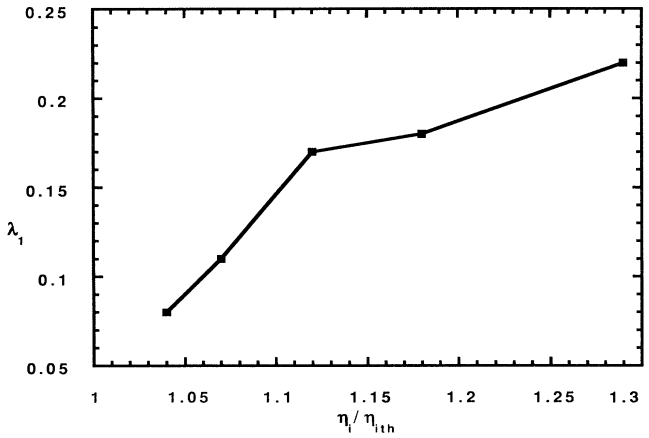


FIG. 4. The largest Liapunov exponent $\lambda_1$ (in units of $c_s/L_n$) as a function of $\eta_i/\eta_{ith}$ for $\varepsilon_n=1$, $\tau=1$, $\eta_{ith}=1.78$ and with an embedding dimension of $D_e=8$.

ic. It is interesting to note that the motion on the high-dimensional attractors appears to be chaotic too, although in this regime a simple quasilinear approximation has been found to adequately reproduce the ion energy transport [12]. However, the turbulence is here weakly chaotic in the sense that the time scale of the exponential separation of nearby orbits is slower than the time scale of the linear instability. The Liapunov exponent generally increases with increasing $\eta_i$, as shown in Fig. 4. The given values of $\lambda_1$ are weakly dependent on the embedding $D_e$, delay $\tau$, etc., but our interest here is in the scaling of $\lambda_1$ with $\eta_i$, and this is independent of the embedding parameters. For the parameter values in Fig. 4, the real frequency as given by Eq. (3) is $\omega_r \approx -0.5$ (in units of $c_s/L_n$, $k^2\rho_s^2=0.1$), i.e., we have $|\omega_r| > \lambda_1$.

In conclusion, low-dimensional chaotic attractors have been observed in the strongly nonlinear regime of toroidal $\eta_i$-mode turbulence. Chaos was also found in the weakly nonlinear regime, but here the attractors were of higher dimension ($>6$). When applied to tokamak equilibria, the model suggests the presence of low-dimensional chaotic attractors preferably in $L$-mode discharges and in the outer part of the good confinement region, while in the flat density regime associated with the core region of $H$-mode discharges, the dynamics is high dimensional. While the detailed results of the calculations presented in this Letter are likely to be model dependent, the qualitative features emphasized in this work, the low- and high-dimensional chaotic attractors occurring in cases of strong and weak nonlinear coupling, respectively, are believed to be generic for the $\eta_i$ modes and possibly for systems of drift-wave type in general. Work is under way to test this hypothesis and to establish the details of the transition from high- to low-dimensional attractors as well as the transition from nonchaotic to chaotic attractors.

The authors would like to thank B. I. Henry and J. Weiland for useful comments on the manuscript. Thanks are also due to H. G. Gustavsson for advice on the numerical algorithms. The calculations in the paper were partly carried out using the Fujitsu VP-100 at the Australian National University Supercomputer Facility.

[1] E. N. Lorenz, J. Atmos. Sci. **20**, 130 (1963).
[2] D. Ruelle and F. Takens, Commun. Math. Phys. **20**, 167 (1971).
[3] R. G. Deissler, Phys. Fluids **29**, 1453 (1986).
[4] A. Brandstäter, J. Swift, H. L. Swinney, A. Wolf, J. D. Farmer, E. Jen, and P. J. Crutchfield, Phys. Rev. Lett. **51**, 1442 (1983).
[5] M. Sano and Y. Sawada, Phys. Rev. Lett. **55**, 1082 (1985).
[6] P. Y. Cheung and A. Y. Wong, Phys. Rev. Lett. **59**, 551 (1987).
[7] P. C. Liewer, Nucl. Fusion **25**, 543 (1985).
[8] C. S. Liu, Phys. Fluids **12**, 1489 (1969).
[9] B. Coppi and F. Pegoraro, Nucl. Fusion **17**, 969 (1977).
[10] W. Horton, D.-I. Choi, and W. M. Tang, Phys. Fluids **24**, 1077 (1981).
[11] A. Jarmén, P. Andersson, and J. Weiland, Nucl. Fusion **27**, 941 (1987).
[12] H. Nordman and J. Weiland, Nucl. Fusion **29**, 251 (1989).
[13] R. E. Waltz, Phys. Fluids **29**, 3684 (1986).
[14] B. B. Kadomtsev, *Plasma Turbulence* (Academic, New York, 1965).
[15] N. H. Packard, J. P. Crutchfield, J. D. Farmer, and R. S. Shaw, Phys. Rev. Lett. **45**, 712 (1980); F. Takens, in *Dynamical Systems and Turbulence,* Lecture Notes in Mathematics Vol. 898, edited by D. A. Rand and L.-S. Young (Springer, Berlin, 1981), p. 366.
[16] P. Grassberger and I. Procaccia, Phys. Rev. Lett. **50**, 346 (1983).
[17] A. Wolf, J. B. Swift, H. L. Swinney, and J. A. Vastano, Physica (Amsterdam) **16D**, 285 (1985).